Bulletin of the Geological Society of Finland, Vol. 94, 2022, pp 145–164 https://doi.org/10.17741/bgsf/94.2.003

Hiekkapohja hydrothermal system – ore mineral, lithogeochemical and paleomagnetic evidence from the Paleoproterozoic Central Finland Granitoid Complex

Esa Heilimo[1*], Sini Halonen[2,3], Satu Mertanen[4], Sami Niemi[5] and Perttu Mikkola[5]

[1]*Department of Geography and Geology, Akatemian katu 1, FI-20014, University of Turku, Finland*

[2]*Oulu mining school, P.O.Box 8000, FI-90014, University of Oulu, Finland*

[3]*Labroc Oy, Tyrnäväntie 12, FI-90400, Oulu, Finland*

[4]*Geological Survey of Finland, P.O. Box 96, FI-02151, Espoo, Finland*

[5]*Geological Survey of Finland, P.O. Box 1237, FI-70211, Kuopio, Finland*

Abstract

The Paleoproterozoic Svecofennian Central Finland Granitoid Complex (CFGC) has been regarded as an area of low mineralisation potential. The Hiekkapohja area, 20 km north-east of the town of Jyväskylä, host a concentration of variable metalliferous showings. Samples from mineralised boulders and outcrops display variable combinations of anomalously high concentrations of Cu, Mo, Zn, Pb, W, Pb, Ag, As, and Au. The area is composed mainly of peraluminous and ferroan granitoids. The dominant porphyritic Hiekkapohja granodiorite (~1.88 Ga) is cross-cut by the equigranular Soimavuori granite of similar age. The porphyritic Lehesvuori granite on the western side of the study area represents marginally older (~1.89 Ga) magmatism. The paragenetic sequence of the ore minerals shows that the Hiekkapohja area has been affected by at least two separate stages of hydrothermal activity. The first mineralisation stage was widespread, crystallising typically chalcopyrite, pyrrhotite, sphalerite, galena, arsenopyrite, magnetite and Ag-bearing minerals. After the first stage, a low temperature oxidising phase formed hematite and marcasite. The second mineralisation stage enclosed low temperature minerals, such as marcasite and native Ag and Ag-minerals, as inclusions inside chalcopyrite, pyrite, pyrrhotite, sphalerite, and arsenopyrite. The mineralised samples typically display signs of K-metasomatism and less commonly signs of propylitic alteration. During the second mineralisation stage the fluid flow was controlled by the dominant 120°–135° trending shear zones. Both the hydrothermal activity and the regional geology indicate that porphyry type ore forming processes have occurred in the Hiekkapohja area. Paleoproterozoic resetting of the remanent magnetisation is further evidence for the role of the hydrothermal system.

Keywords: Central Finland Granitoid Complex, hydrothermal, mineralisation, geochemistry, paleomagnetism, Paleoproterozoic

*Corresponding author (e-mail: esa.heilimo@utu.fi)

Editorial handling: Shenghong Yang (e-mail: shenghong.yang@oulu.fi)

1. Introduction

Porphyry Cu-Mo deposits can be found from both active and extinct volcanic arc settings. The deposit type is more abundant in Phanerozoic than in Proterozoic, and the oldest economic ore deposits are Paleozoic in age (Kesler & Wilkinson 2008). However, a possible exception is the Paleoproterozoic Aitik deposit in northern Sweden (Wanhainen et al. 2006).

The Paleoproterozoic Central Finland Granitoid Complex (hereafter CFGC) is composed mainly of synorogenic granitoids formed in a convergent setting (e.g. Lahtinen et al. 2005) and, based on this tectonic setting, could be regarded as having potential for porphyry type deposits. However, only one deposit within the CFGC, the Kopsa (Au-Cu) deposit, has thus far been more intensively studied in this respect (Rasilainen et al. 2014; Fig. 1). Other potential porphyry-type Svecofennian mineral targets outside the CFGC include Kedonojankulma (Cu-Mo-Au) in Southern Finland and Lammuste (Cu-Au) in Central Finland (Nurmi 1982, Tiainen et al. 2013, Solismaa et al. 2018; Fig. 1).

The CFGC generally displays limited signs of mineralisation, the most notable exception being the Hiekkapohja area (also known as Palokka) located in the SE part of the CFGC, 20 km north-east of Jyväskylä (Fig. 1). In this area, numerous mineralised boulders and outcrops are known from target scale studies carried out in 1980s by Geological Survey of Finland and Outokumpu Ltd. (Ikävalko 1981, 1983, 1984, 1986a, b, Hangala 1982, Nurmi 1982, Rantala 1982, Nenonen & Huhta 1983, Laitakari 1985). The main incentive for the earlier research activity were high-grade layman's samples variably enriched in Cu, Mo, Zn, W, Pb, Ag, As, and Au. The source for a number of the mineralised boulders remained unclear. During the deglaciation, the Hiekkapohja area was located in a region of passive/dead ice and, thus, short glacial transport distances would be expected.

Mineralised outcrops were typically found within shear zones. Based on the dominant ore minerals, Laitakari (1985) divided the outcrops into two types: (1) arsenopyrite-chalcopyrite type and (2) sphalerite-galena type (showing Ag contents up to 151 ppm). Due to the limited expectations, only two targets, Riuttamäki and Karhujärvi were drilled (Fig. 2; op. cit.). In both locations, the country rocks are porphyritic granodiorite and quartz diorite that host a shear zone with some 20–40 cm wide zones of massive sulphide. In Riuttamäki one-meter drill core intersection contained 0.7 wt.% Cu, 230 ppm Zn, and 17 ppm Ag (Ikävalko 1981).

In this study, we aim to explain the nature and origin of the mineralised rocks and related geological features in the Hiekkapohja area, which does not significantly differ from its barren surroundings. We also propose a possible mineralisation type for the area, explaining the variable enrichment combinations of multiple elements. We emphasize the hydrothermal alteration events and the factors controlling the fluid activity. Our research material includes bedrock and boulder observations, thin sections, whole-rock geochemical data, mineral chemistry, ground geophysical surveys (Heilimo & Niemi 2015), and paleomagnetic data. Whole-rock and mineral geochemical, as well as ore mineralogical, data are from the unpublished MSc thesis by Halonen (2015).

2. Geological setting

The CFGC forms the core of the Paleoproterozoic (Svecofennian) crustal domain in Finland. The evolution of the Svecofennian orogeny (1.93–1.78 Ga) has been explained as a complex accretionary process involving several subduction zones and amalgamation of island arcs and other crustal blocks with the Archean Karelia province (e.g. Lahtinen et al. 2005, Nironen 2017). Based on geochemical characteristics the older (1.93–1.91 Ga) Svecofennian magmatism is regarded as primitive island arc type (Nironen 1997). The younger, mature arc type Svecofennian magmatism commenced at 1.89 Ga (cf. Lahtinen et al. 2005,

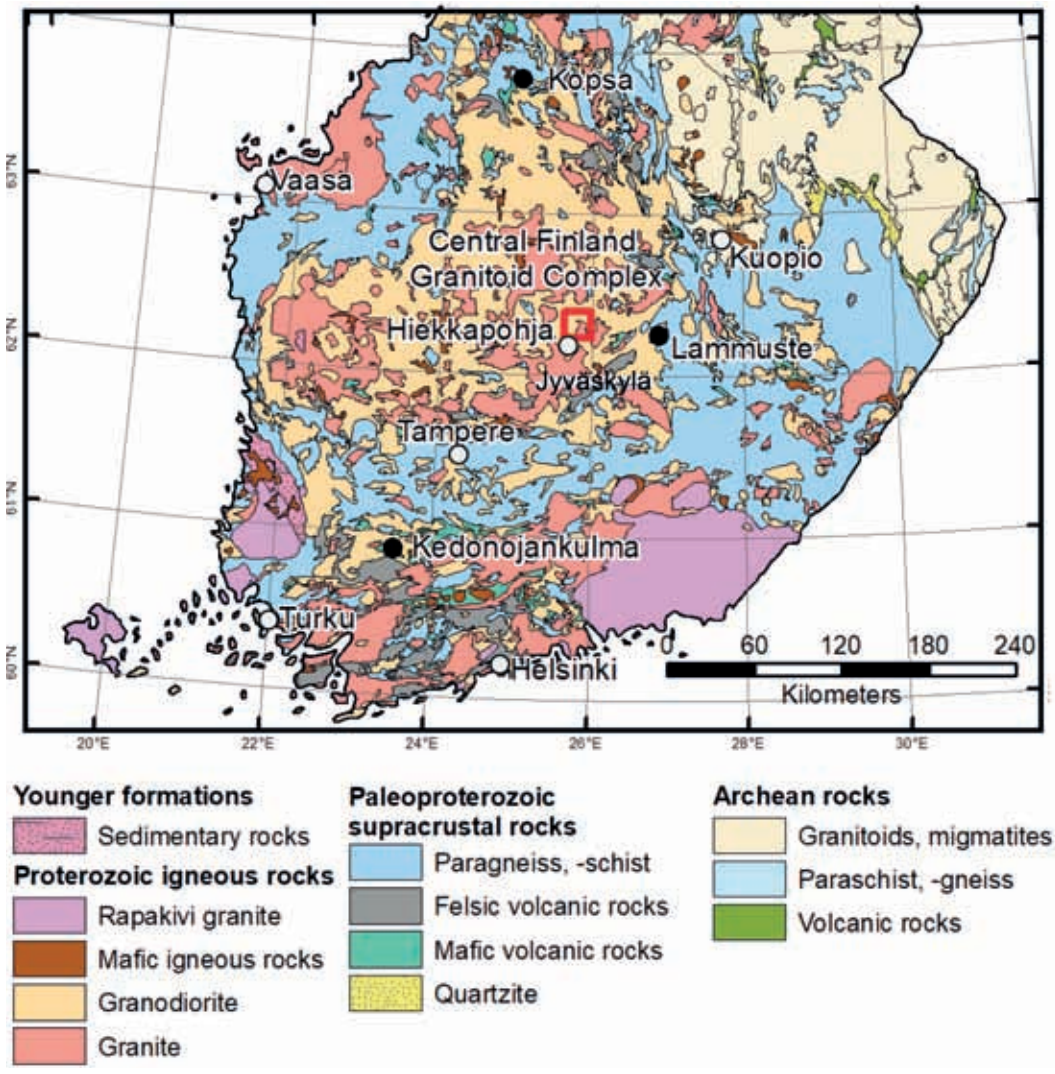

Figure 1. Location of the study area (map modified from Nironen et al. 2016).

Nironen 2017, Mikkola et al. 2018). The CFGC formed during this younger main phase of the Svecofennian magmatism. The calc-alkaline continental arc-type magmatism continued for ~20 Ma and produced both the voluminous plutonic rocks of the CFGC as well as the intrusions in the surrounding paragneiss belts. Related volcanic rocks are preserved mainly as a discontinuous belt along the boundaries of the CFGC. The composition of the plutonic rocks does not show abrupt time dependant changes. Instead, there is a gradual transition from quartz diorites (Vaajakoski lithodeme, Jyväskylä suite) and porphyritic granodiorites (Muurame lithodeme, Jyväskylä suite) to leucocratic granites (Soimavuori lithodeme, Oittila suite). This compositional change has been interpreted as a sign of maturing of the continental arc, and it could be partly attributed to exhumation of the crust (Heilimo et al. 2018, Mikkola et al. 2018). During the late stages of calc-alkaline magmatism, the CFGC and its surroundings were intruded by a bimodal diorite–granitoid suite displaying A-type geochemical characteristics (Rautalampi and Saarijärvi suites).

In the study area these rocks yield ages around 1880–1875 Ma (Nironen et al. 2000, Rämö et al. 2001, Virtanen & Heilimo 2018) and are spatially associated with crustal-scale shear zones. The shear zones plausibly facilitated ascent of the granitic magmas in a transtensional setting. The Lehesvuori granite located in the western part of the study area (see Fig. 2), has been dated at 1891 ± 5 Ma (Lahtinen et al. 2016). Sm-Nd isotopes reveal signs of older crustal inheritance in this granite, as its depleted mantle model age is 2.41 Ga (Huhma 1986).

The bedrock of the CFGC is characterised by major shear zones (see Fig. 2) divided into three groups from the oldest to the youngest: 1) 20°–40° trending, 2) 120°–135° trending, and 3) 0° trending. The first group could be related to the extensional or transtensional stage at ca. 1880–1875 Ma (Nironen 2003, Mikkola et al. 2018). In Hiekkapohja area, the 120°–135° trending shear system is the most prominent, whereas movements in stage 3 are minor. The timing of the two younger groups is challenging, but group 2 could be temporally close to the group 1 due to ambiguous crosscutting relationships (Mikkola et al. 2018).

3. Methods

Mapping and surveying

'Central Finland's ore potential estimation' -project (2012–2015) produced a 1:200 000 bedrock map along the south-eastern boundary of the CFGC (Mikkola et al. 2016, 2018). In addition, the ore potential areas were selected for a more detailed work, and the Hiekkapohja area was mapped as a part of the project. The objective was to identify the possible differences compared to the rock types of the surrounding areas. The results of the geophysical ground surveys (magnetic profiles) and geochemical studies of the till samples collected along a profile transecting the core of the area have been reported in Heilimo & Niemi (2015).

Analytical methods

A new geochemical dataset with 47 whole-rock samples taken from boulders and outcrops was compiled. The dataset contains both new samples and reanalysed older layman´s samples received by the Geological Survey of Finland and Outokumpu mining. All samples were analysed with a wavelength-dispersive X-ray fluorescence (XRF) spectrometer from powder pellets (Labtium code 175X with carbon analyse 811L), and 16 were further analysed by inductively coupled plasma mass spectrometry (ICP-MS) for additional trace elements (Labtium method 308PM). Most of the samples (n=33) were analysed also with an inductively coupled plasma optical emission spectrometry (ICP-OES) using partial leaching (Labtium method code 704/705 for the platinum group elements and/or gold, and Labtium method 511PM for the rest of the elements). Additionally, three samples from the dataset of Rasilainen et al. (2007) have been used. All analytical data and the methods used are listed in Electronic Appendix A.

Mineral chemistry

Mineral chemical analyses were performed at the Geological Survey of Finland to identify ore minerals. Scanning electron microscope energy dispersive analyses (SEM-EDS) were conducted usingINCA software. Beam accelerating voltage was 20 kV and current 1.5 nA. A detailed description of this method is available in Lehtonen & Kortelainen (2010). Some additional SEM-EDS and electron probe microanalysis (EPMA) studies were performed at the University of Oulu. EPMA analyses were done to identify the silver bearing minerals, and these data are available in the unpublished MSc thesis by Halonen (2015).

Paleomagnetic methods

A total of 42 samples collected from six different locations covering the main rock types of the area as well as the regions of weakest and

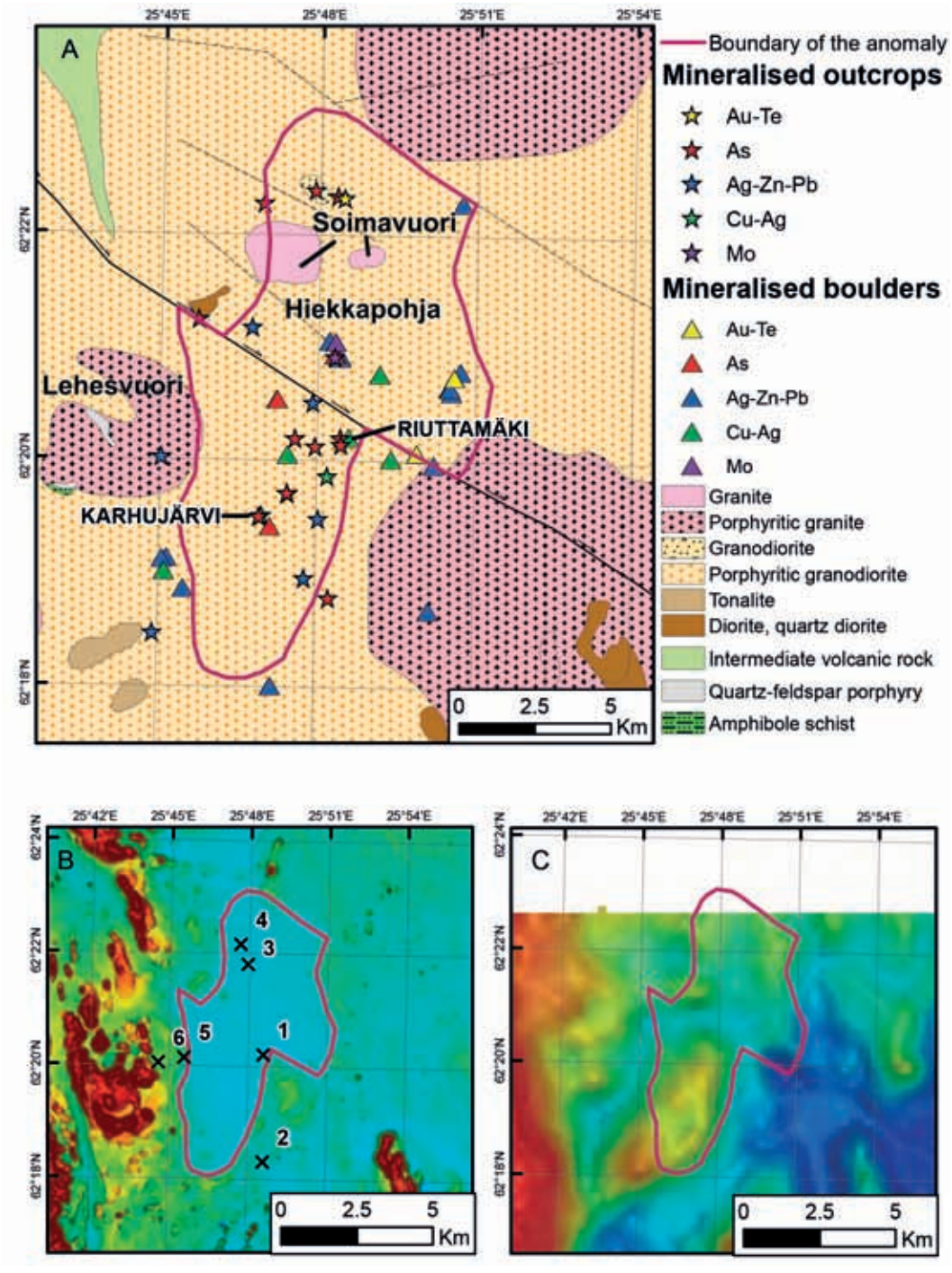

Figure 2. a) Bedrock map of the Hiekkapohja area (modified from Mikkola et al. 2016) with the known mineralised occurrences and the outline of the aeromagnetic low (solid purple line). b) Aeromagnetic map of the Hiekkapohja area, with the numbers indicating the paleomagnetic sample sites; 1) Riuttamäki Cu-Zn-Ag sulphide bearing porphyritic granodiorite, 2) Ankeriasjärvi porphyritic granodiorite, 3) Soimavuori granite, 4) Halsvuori porphyritic granodiorite and granitic vein, 5) Lehesvuori porphyritic granite, 6) Lehesvuori quartz-feldspar porphyry. c) Regional Bouguer residual anomaly map highlighting near surface density variations.

strongest magnetic anomaly and most promising mineralisations, were studied for paleomagnetic and petrophysical properties. All samples were collected using a portable mini drill, and oriented with magnetic and/or sun compass. The diameter of the retrieved cores is 2.5 cm and the length of the samples varied from 5 to 10 cm. The applied paleomagnetic method is described in Electronic Appendix B.

4. Results

4.1 Geophysics

In aeromagnetic data, the most prominent feature of the Hiekkapohja area is a negative anomaly, ca. 9 x 4.5 km in size (Fig. 2b), hosting the majority of the known ore indications. The anomaly area is crosscut by a dextral fault. Based on the orientation and the sense of the movement, the fault can be regarded as belonging to the second, 120°–135° trending generation of the main shear zones of Nironen (2003). On the residual Bouguer anomaly map, the Hiekkapohja area is located in a field of medium to high residual Bouguer values (-0.6 – 0 mgal, Mikkola et al. 2016) between a large positive anomaly associated with a gabbro-diorite intrusion to the west, and elongated lows caused by a major fault zone to the east (Fig. 2b, c; the gabbro-diorite intrusion is outside the area of Fig. 2a). No feature resembling the shape of the aeromagnetic low can be observed from Bouguer residual data (Fig. 2b, c). Ground geophysical surveys carried out at the Riuttamäki deposit revealed that the mineralisations can be identified from magnetic and electromagnetic profiles (Heilimo & Niemi 2015). Despite explicit processing trials, the small known mineralisations could not be located using the low altitude aerogeophysical data. The lack of moderate to high magnetic values in ground based geophysical and aeromagnetic data indicate that all deposits in the Hiekkapohja area are likely to be small.

4.2 Bedrock mapping

The dominant rock type within the aeromagnetic low area is a deformed medium-grained potassium feldspar porphyritic granodiorite (Muurame lithodeme, Jyväskylä suite) that does not differ at outcrops from the corresponding rocks in surrounding areas (Fig. 2; Mikkola et al. 2016). Hereafter, this rock type is referred to as Hiekkapohja granodiorite. The age of the porphyritic granodiorite is 1882 ± 4 Ma (authors' unpublished U-Pb data), which is a typical age for the Muurame lithodeme of Heilimo et al. (2018). The porphyritic granodiorite is relatively homogeneous and devoid of inclusions, only a small number of paragneiss and amphibolite xenoliths were observed. The porphyritic granodiorite is locally crosscut by equigranular, pink granite veins, which are in some cases pegmatitic and do not display uniform orientation (Fig. 3a). Based on bedrock surface samples obtained during basal till sampling, there is also a small quartz diorite intrusion within the granodiorite (Heilimo & Niemi 2015), but this is not the main rock type on any of the mapped outcrops.

The potassium feldspar porphyritic (<1.5 cm) Lehesvuori granite (1891 ± 5 Ma, Lahtinen et al. 2016) on the western edge of the aeromagnetic low has relatively undeformed appearance at outcrops (Figs. 2, 3; paleomagnetic sites 5 and 6). The Lehesvuori granite is crosscut by at least two pink granite dykes with hypabyssal appearance that are correlated with the Soimavuori granite of the Oittila suite (Heilimo et al. 2018; Fig. 3). The maximum width of these dykes is 130 m. Despite their unfoliated field appearance, both the Lehesvuori and Soimavuori granites show signs of deformation, such as recrystallisation and foliation in the microscopic scale.

Two rounded granite intrusions called Soimavuori granite are located in the northern part of the Hiekkapohja area. The larger one of these has a diameter of 1.3 km (Fig. 2a). These weakly foliated, even-grained, pale grey intrusions are the youngest granitoids in the area according to Heilimo et

Figure 3. a) Soimavuori granite hosting an enclave xenolith of the potassium feldspar porphyritic granodiorite, which is the dominant rock type in Hiekkapohja area. The enclave also contains equigranular granite veins. b) Pink hypabyssal granite dyke cross-cutting the Lehesvuori granite.

al. (2018). In addition to the two intrusion, these granites cross cut the surrounding Hiekkapohja granitoid as dykes. Age determination of a sample representing this granitoid type yielded 1879 ± 4 Ma (authors' unpublished U-Pb data).

4.3 Geochemistry

We have divided the granitoid samples into two groups: (1) the porphyritic Hiekkapohja granodiorite belonging to the Muurame lithodeme, Jyväskylä suite, and (2) the even-grained, younger Soimavuori granite belonging to the Oittila suite. The less common quartz diorites of the Vaajakoski lihodeme and the Lehesvuori granite belong to the Jyväskylä suite. This division has been proposed by Heilimo et al. (2018) after the comprehensive fieldwork in the area (Mikkola et al. 2016). There are no significant geochemical differences between the unmineralised samples from the aeromagnetic low area and outside of it. However, the mineralised and clearly altered samples typically show indications of K- metasomatism and, in some cases, signs of propylitic alteration can be found. In general, the medium K-metasomatism is more common inside the local aeromagnetic low. Figure 4 summarises the elemental composition of the studied samples, some of the major element and selected trace element compositions are presented in the Figure 5. The complete dataset is available in the Electronic Appendix A.

4.3.1 Geochemistry of the non-mineralised samples

The major element compositions of Hiekkapohja and Soimavuori granitoids are mainly similar, although the samples from the Soimavuori granite have on average marginally higher SiO_2 contents (69.00–75.80 wt.%) compared to the Hiekkapohja granodiorite (64.90–75.80 wt.%). Both granitoids are mainly peraluminous and ferroan without major outliers (Fig. 4). Both granitoids show calc-alkalic characteristic (Frost et al. 2001) as well as relatively high K_2O contents at given SiO_2 contents. The chondrite-normalised REE patterns for the Hiekkapohja and Soimavuori granitoids display similar enrichment of LREE over HREE $(La/Yb)_N = 7.0–44.7$ (Fig. 6).

The Lehesvuori granite and the hypabyssal felsic dyke as well as the surrounding porphyritic granodiorite do not differ significantly from the surrounding granitoid rocks in terms of major elements composition. However, the chondrite-normalised REE patterns of the hypabyssal felsic rock are flat, $(La/Yb)_N = 1.8–9.8$ (Fig. 6), and

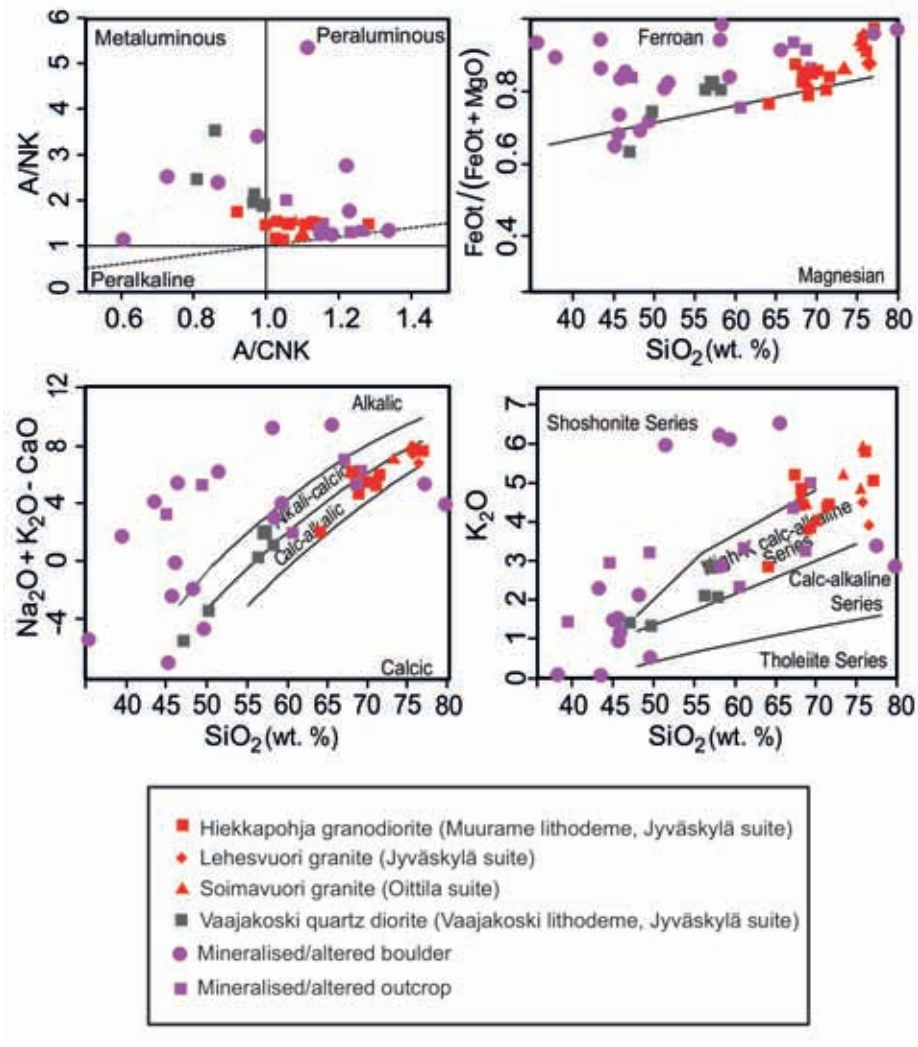

Figure 4. Classification Harker diagrams of the studied samples from the Hiekkapohja area. Alumina saturation index diagram A/CNK vs. A/NK, FeOt/(FeOt+MgO) vs. SiO_2 after Frost et al. (2001), MALI diagram Na_2O+K_2O-CaO vs. SiO_2 after Frost et al. (2001), K_2O vs. SiO_2 the series lines after Peccerillo & Taylor (1976).

it displays a significant negative Eu-anomaly (Eu/Eu* ≈ 0.20). The quartz diorites in the study area are typical members of the Vaajakoski lithodeme (Heilimo et al. 2018). They are metaluminous and ferroan, displaying alkali-calcic compositions in the MALI diagram (Fig. 4). The SiO_2 content varies between 47.10 wt.% and 58.20 wt.%, and other major elements show a clear correlation with SiO_2 content.

4.3.2 Geochemistry of mineralised and altered samples

Whole rock chemistry shows elevated concentrations of base and precious metals in the mineralised and altered samples. The mineralised and altered samples originally represent all the rock types observed in the region. They differ compositionally from the un-mineralised samples due to clear scatter in SiO_2 and K_2O contents, probably due to hydrothermal fluid activity. The general compositions vary between metaluminous and peraluminous, and alkalic to calc-alkalic (Fig. 4; Electronic Appendix A). The SiO_2 content varies between 19.80 wt.% and 79.90 wt.%. The highest K_2O contents are equivalent to the shoshonitic series (Fig. 5). Contents of the relatively mobile trace elements (Sr, Rb) vary significantly, and are partly lower than those observed in the unaltered samples.

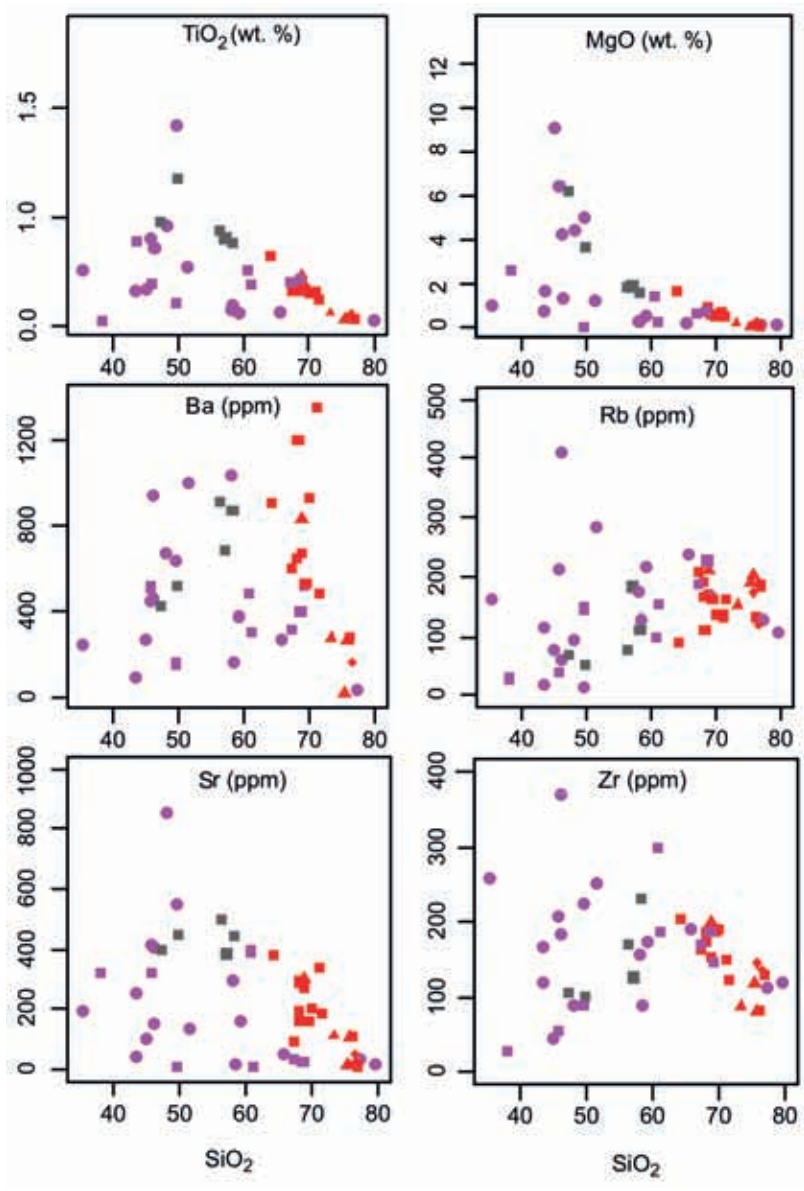

Figure 5. Harker diagrams of the studied samples from the Hiekkapohja area. On vertical axes TiO_2, MgO, Ba, Rb, Sr, and Zr (symbols as in Figure 4).

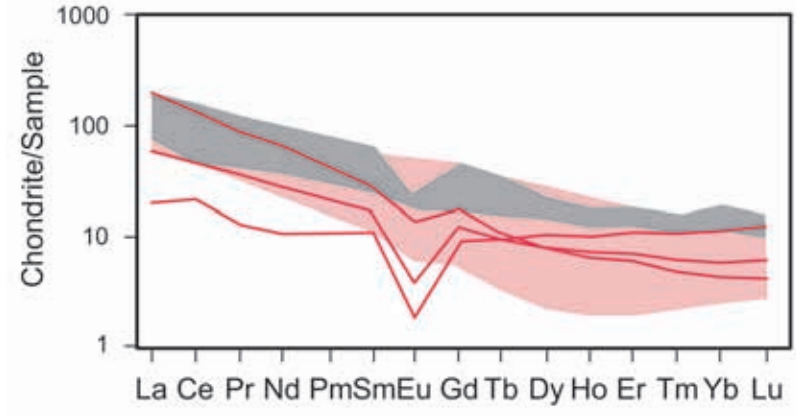

Figure 6. Chondrite normalised REE patterns of the studied samples (normalising values from Boynton 1984). Pink field represent samples from Hiekkapohja granodiorite and Soimavuori granite. Gray field represents Vaajakoski quartz diorite samples. Red lines represent samples from Lehesvuori, the flattest REE pattern is from the felsic hypabyssal dyke from Lehesvuori.

The analytical results for base and precious metals from Hiekkapohja are summarised in Electronic Appendix A. The copper contents are elevated in some of the samples, with the highest concentration being up to 2.1 wt.% in a mineralized amphibolite boulder sample (K2693). The highest reported concentrations from the Riuttamäki drill core sample are 0.7 wt.% Cu, 230 ppm Zn, and 17 ppm Ag (Ikävalko 1981). In the granitoid samples from the Hiekkapohja area, there is generally positive correlation between Ag, and Cu and Au contents, and between W and Cu contents, although scatter exists (Fig. 7). The observed degree of K-metasomatism is related to the Cu content. Mo is typically low in the studied samples, but mineralised porphyritic granite boulder sample (K3678) contains 2376 ppm of Mo. Zinc contents are clearly above analytical detection limits in all samples, with the highest concentration being 5.4 wt.% in a mineralised, mylonite granite boulder sample (K_3969). Additionally, five samples have Zn concentration >1 wt.%. Unlike Ag, Au, and W, Zn content does not correlate significantly with the Cu content. Propylitically altered granite boulder sample (TOS$-2014-187.1) contains the highest W concentration, 327 ppm, but the rest of the samples do not display elevated contents. Silver, when above detection limit, displays values from 1.5 to 151 ppm. Nearly 100 ppm concentrations of Ag are found in the amphibolite and granite boulder samples, (K_2438, K_4338 and K2693) as well as in an amphibolite outcrop outside of the aeromagnetic low (K_2018). Amphibolite samples (K5366 and K2018) from outcrops outside the aeromagnetic low, contain over 100 ppb Au, representing the highest observed Au values.

4.4 Ore mineralogy

Mineralogical studies were undertaken on 19 samples from the study area, five of these originate from outcrops and 14 from boulders (Table 1). The samples represent different rock types (Fig. 8a), including the porphyritic granite of the Muurame lithodeme, undefined amphibolite that is possibly a deformed fine-grained variant of the Vaajakoski lihodeme, as well as gneisses, and mica schists. The observed ore mineralogy does not display correlation with the host rock type. Ore mineral assemblages, grain size, and mineral textures vary significantly between samples, as sulphide minerals appear either as massive (Fig. 8b), as dissemination, or as veins with variable mineralogy (Fig. 8c). Intergranular texture is the typical primary feature, whereas a bird eye-texture caused by chalcopyrite disease is observed as a secondary feature. Another typical feature is the colloform alteration of pyrrhotite and chalcopyrite to marcasite (Fig. 8e, f), although the quantity of each mineral varies between samples.

The most common ore mineral is chalcopyrite, and other main ore minerals include pyrite, pyrrhotite, sphalerite, and arsenopyrite. Pyrite occurs in almost every sample, but it is rarely the main sulphide mineral. Observed oxide minerals include magnetite, hematite, cassiterite, ilmenite, and rutile. Rare sulfosalt minerals, such as matildite, are also found in the amphibolite samples (K_5366, K2693; Table 1). The main ore minerals do not contain significant amounts of Ag as trace element. Instead, a wide range of silver bearing minerals are observed, the most common one being acanthite (Ag_2S) in granitoid boulder samples (K_2438, K3678, 79_8379oku, 71_VM_2oku, 20112473) as well as in amphibolite and diorite samples (Table 1; Fig. 9). Other silver bearing minerals are matildite ($AgBiS_2$), stephanite (Ag_5SbS_4), argentinopyrite ($AgFe_2S_3$), pyragyrite (Ag_3SbS_3), and hessite (Ag_2Te). Small, metallic native grains of silver are also present in the samples.

4.5 Paleomagnetism

Petrophysical properties (density, susceptibility and remanent magnetization) of all the studied sites are given in Table 2. Results of the paleomagnetic studies, which show the remanence directions after multicomponent analyses, are shown in Table 3. Only in sites 3 (Soimavuori) and 4 (Halsvuori) a stable remanence direction was found in several

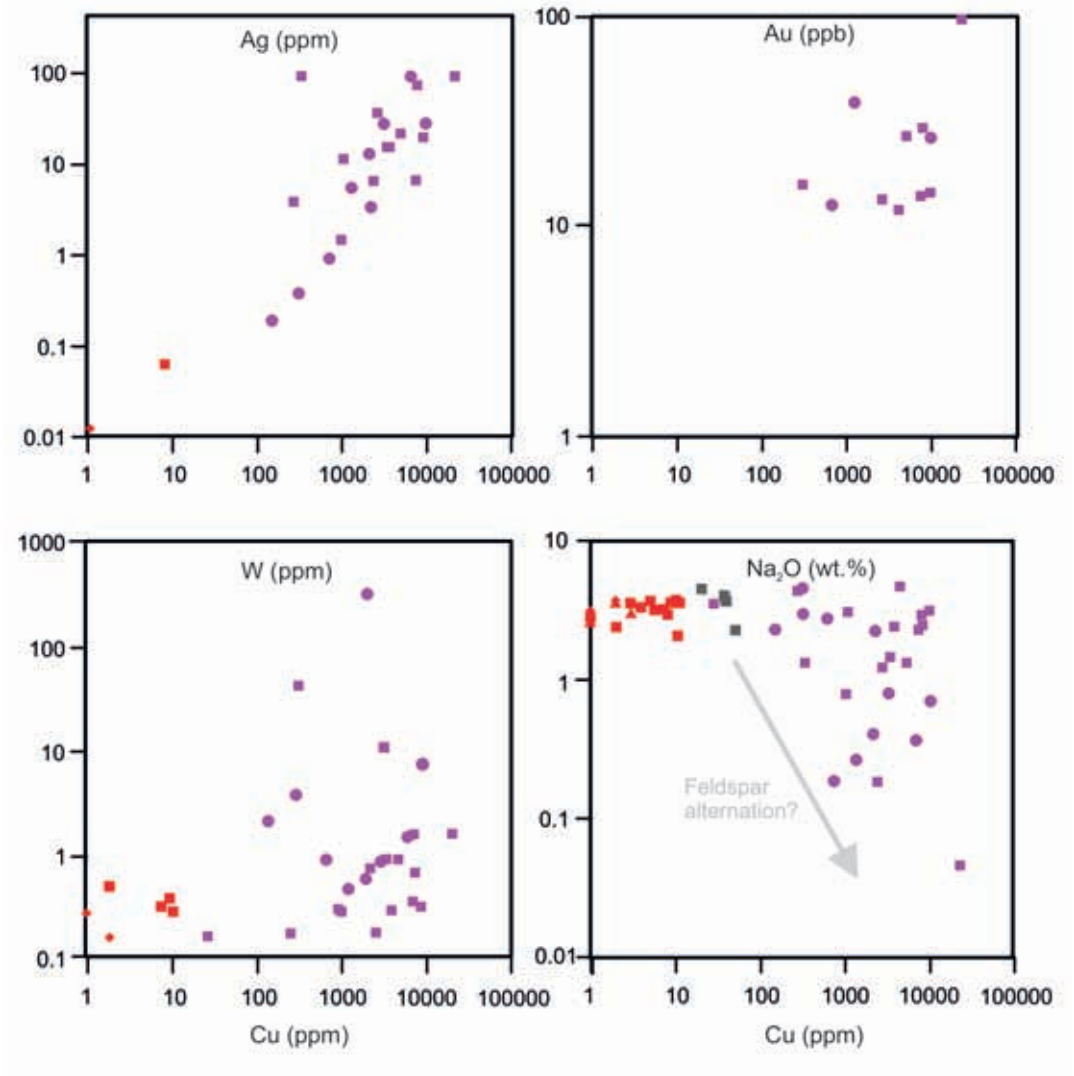

Figure 7. Logarithmic Cu diagrams of the studied samples from the Hiekkapohja area. On vertical axes Ag, Au, W, and Na_2O (symbols as in Figure 4).

samples. The remanence directions of the other sites are too scattered for determining consistent directions. The description of all sites can be found from Electronic Appendix C.

Five samples out of the six studied representing the Soimavuori granite display a stable remanence direction with a NW pointing declination and an intermediate inclination, the direction typical for a Svecofennian age formations. Based on high coercivities during alternating field (AF) demagnetization and on thermal demagnetization that shows unblocking of remanence at temperatures of 300–370°C, the remanence is carried by pyrrhotite (Fig. 10). Likewise, in Halsvuori a consistent NW pointing moderate inclination remanence direction was isolated in all six studied porphyritic granodiorite samples. The same direction was also isolated in four out of six samples from the cross-cutting veins (Table 3). Like in Soimavuori granite this stable paleomagnetic direction was isolated in temperatures between 320-370°C (Fig. 10), indicating pyrrhotite as the remanence carrier.

Table 1. Summary of the dominant ore mineralogy of the studied sample based on scanning electron microscope as energy dispersive analyses (SEM-EDS).

Sample lithology	Sample number	Chalcopyrite ($CuFeS_2$)	Sphalerite (ZnS)	Pyrite/Marcasite (FeS_2)	Pyrrhotite ($Fe_{1-x}S$)	Arsenopyrite (FeAsS)	Magnetite (Fe_3O_4)	Galena (PbS)	Ilmenite (Fe_2TiO_3)	Rutile (TiO_2)	Argentopyrite ($AgFe_2S_3$)	Matildite ($AgBiS_2$)	Greenockite (CdS)	Hessite (Ag_2Te)	Acanthite (Ag_2S)	Bornite (Cu_5FeS_4)	Graphite (C)	Löllingite ($FeAs_2$)	Roquesite ($CuInS_2$)	Cassiterite (SnO_2)	Covellite (CuS)	Cobaltite (CoAsS)	Hematite (Fe_2O_3)	Bismuth (Bi)	Pyrargyrite (Ag_3SbS_3)	Stannite (Cu_2FeSnS_4)	Stephanite (Ag_5SbS_4)	Silver (Ag)
Amphibolite	K_5366	x	x	x								x	x															
Amphibolite	K_2018	x	x	x	x	x		x	x																			x
Alkali granite	384_76oku	x	x	x										x														
Alkali granite	2525_oku	x	x	x	x	x			x	x	x																	x
Sillimanite granite	82_10912oku	x	x	x	x	x												x										
Granite mylonite	K_3969	x	x	x	x	x		x																				x
Granite	K_2438	x						x							x													
Epidote-amphibolite	K2693	x	x	x		x						x			x													
Porphyritic granite	K3678	x	x					x							x	x	x											
Granite	80_10528oku	x	x	x	x		x											x										
Porphyritic granite	79_8379oku	x	x			x	x					x			x				x	x			x					
Granite	78_89oku	x	x	x										x					x	x	x							
Syenite	72_758oku	x	x	x		x	x					x					x			x		x						
Granite	71_63oku	x	x	x		x																		x				
Syenite	71_784oku	x	x	x	x						x														x	x		
Syenite	71_VM_2oku	x	x	x	x			x							x												x	x
Diorite	427_OKU	x		x	x										x													
Sericite granite	20112473	x						x							x		x											
Biotite-hornblende gneiss	86_327_oku	x	x	x	x																							

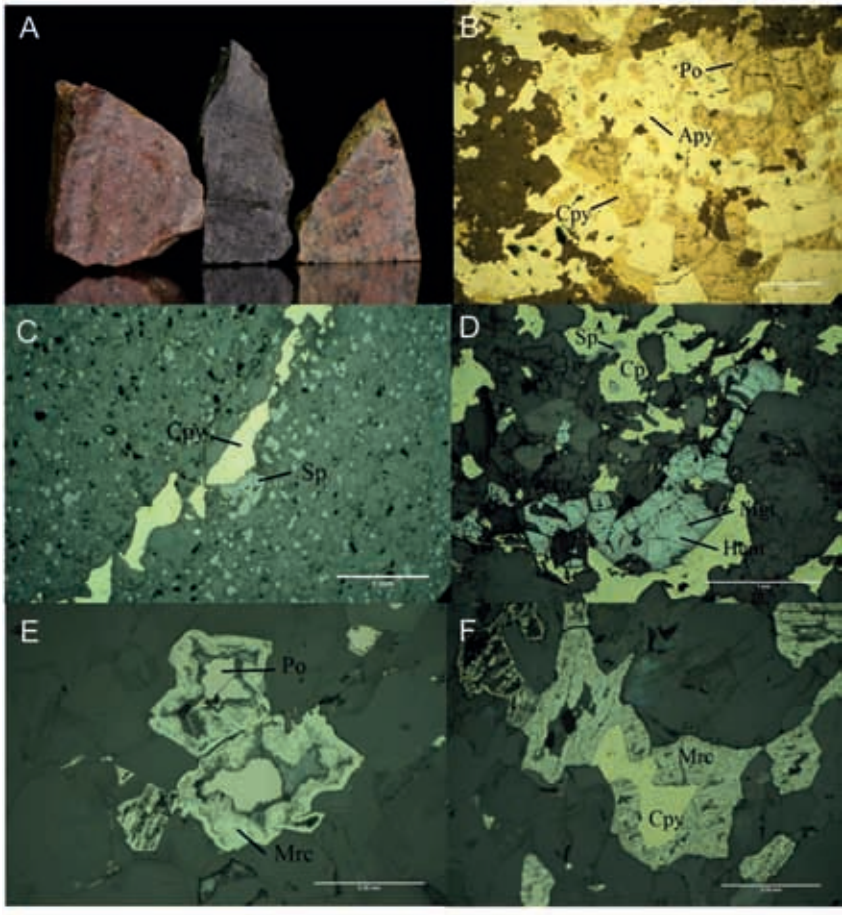

Figure 8. a) Mineralised hand samples from the Hiekkapohja area representing the different mineralised rock types, from left to right: equigranular granite, amphibolite and porphyritic granite (height of the amphibolite is 8 cm). b) Massive texture of pyrrhotite (Po), chalcopyrite (Cpy) and arsenopyrite (Apy) in sillimanite granite sample (82_10912oku). High concentration of silver, 96 ppm, was recorded in this sample. c) Disseminated sphalerite (Sp) and a chalcopyrite-sphalerite vein in diorite sample (K_5366). d) Magnetite (Mgt) partly altered to hematite (Hem), chalcopyrite (Cpy) and sphalerite (Sp) as inclusion in chalcopyrite in porphyritic granite (sample 79_8379oku). e) Pyrrhotite altered to marcasite (Mrc) in biotite-hornblende gneiss boulder (86_327oku). f) Chalcopyrite altered to marcasite from the boundaries in biotite-hornblende gneiss boulder (op. cit.). All the microscope photos (b-f) with reflective light and parallel nicols.

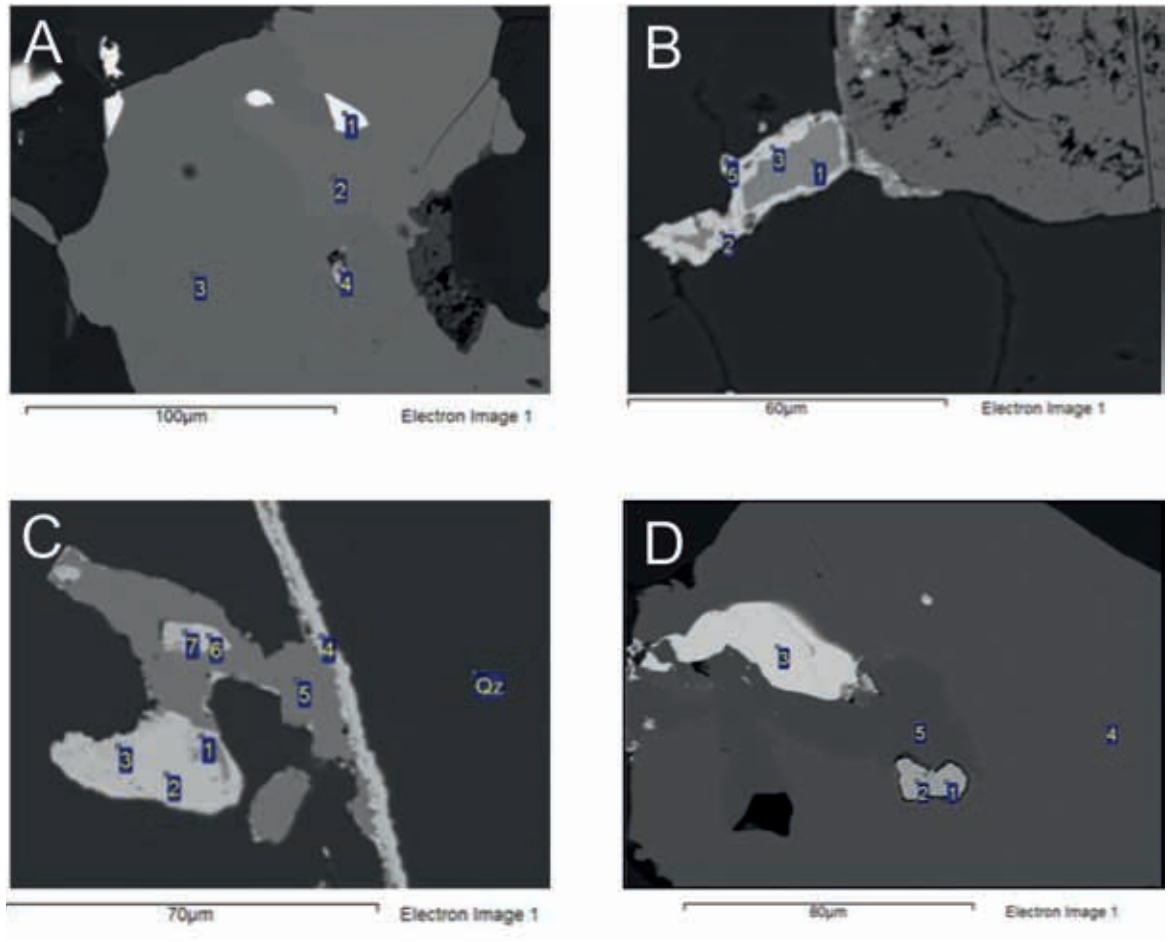

Figure 9. Backscattered electron (BSE) images of Ag-bearing minerals in the Hiekkapohja area. a) Granite boulder (71_784oku): 1 – galena, 2 – chalcopyrite, 3 – pyrite, 4 – Argentopyrite inclusion ($AgFe_2S_3$). b) Porphyritic granite boulder (79_8379): 1 – sphalerite, 2,3,5 – acanthite (Ag_2S). c) Porphyritic granite boulder (K3678): 1,3 – acanthite, 2,4 – galena, 5 – chalcopyrite, 6 – galena inclusion, 7 – acanthite. d) Amphibolite (K_2018): 1,2 – native silver inclusion, 3 –galena inclusion, 4 – chalcopyrite, 5 – pyrite.

5. Discussion

5.1 *Mineralogical evidence for fluid activity stages*

We propose that the mineralogical evidence indicates at least two fluid pulses, with an intermediate period of oxidising conditions and low temperatures, possibly related to supergene processes (Fig. 11). The intensity and type of alteration vary between the samples, but typically low to medium K-metasomatism and, in places, propylitic alteration are present. Both types of alterations might have caused the depletion of Na_2O in the mineralised samples (Fig. 7).

Chalcopyrite, pyrrhotite, sphalerite, pyrite, arsenopyrite, and galena crystallised in variable amounts during the first stage. The first stage mineralisation event in the Hiekkapohja area is widespread and was likely related to an extensive alteration system. The subsequent low temperature -oxidising phase, causing the alteration of pyrrhotite to marcasite, was observed in several granitoid boulder samples (Fig. 8e, f) and in one amphibolite outcrop sample. The formation of marcasite as colloform texture is a sign of very low,

Table 2. Petrophysical properties as arithmetic means of the six paleomagnetic sampling sites.

Site	Area	Sample type	Unit	Coordinates (WGS84)		n	Density	Susc.	Reman.	Q value	Decl	Incl.	α95	k
				x	y		(kg/m^3)	(x 10^{-6} SI)	(mA/m)		(°)	(°)	(°)	
Site 1	Riuttamäki	Granodiorite, mineralised sulphides	Sulphide bearing, Hiekkapohja granodiorite, Muurame lithodeme	62.33673°	25.80955°	6	3199	2538	3199,3	20,3	219,2	65,9	54,7	2,5
Site 2	Ankeriasjärvi	Porphyritic granodiorite	Muurame lithodeme	62.30507°	25.81033°	6	2668	241	2,0	-	33,3	64,5	6,0	125,2
Site 3	Soimavuori	Granite	Soimavuori lithodeme	62.36338°	25.79915°	6	2647	193	1,8	-	15,7	77,7	25,2	8,0
Site 4, samples 1-6	Halsvuori	Porphyritic granodiorite	Muurame lithodeme	62.36938°	25.7943°	6	2668	203	1,3	-	349,5	48,8	12,4	29,9
Site 4, samples 7-12	Halsvuori	Granitic vein	Soimavuori lithodeme	62.36938°	25.7943°	6	2605	76	1,1	-	21,9	70,5	16,3	17,8
Site 4, mean 1-12	Halsvuori	Porphyritic granodiorite + granite vein	Mixed	62.36938°	25.79430°	12	2639	144	1,2	-	0,1	60,4	11,8	14,6
Site 5	Lehesvuori	Porphyritic granite	Lehesvuori lithodeme	62.33573°	25.75932°	6	2608	6406	57,1	0,2	149,2	85,9	9,1	55,1
Site 6	Lehesvuori	Quartz-feldspar porphyry	Lehesvuori lithodeme	62.33412°	25.74307°	6	2606	2909	39,4	0,4	131,5	75,7	17,8	15,1

Note: n is the number of samples, Susc. is magnetis susceptibility, Reman. is intensity of remanence , D is declination and I is inclination of remanence, α95 is the radius of the circle of 95 % confidence, k is Fisher's (1953) precision parameter.

Table 3. Paleomagnetic results from Soimavuori and Halsvuori.

Site/Sample	Rock type	Unit	N/n	D	I	α95	k	Plat	Plong	A95	K
Soimavuori, Site 3											
Mean of site 3	Granite	Soimavuori lithodeme	5/7	346,0	46,2	12,2	40,0	54,5	227,4	13,4	33,7
Halsvuori, Site 4											
Mean of samples 1-6	Porphyritic granodiorite	Hiekkapohja granodiorite, Muurame lithodeme	6/11	334,8	36,1	15,3	20,1	44,5	240,7	16,1	18,2
Mean of samples 7-12	Granitic vein	Soimavuori lithodeme	4/5	329,7	49,1	24,5	15,0	52,2	253,2	29,0	11,0

Note: N/n is the number of samples/cylinders where the remanence component was isolated. D is declination and I is inclination of the remanence. α95 is the radius of the circle of 95 % confidence, k is Fisher's (1953) precision parameter. Plat and Plong are the paleolatitude and paleolongitude for the Virtual Geomagnetic Poles. A95 is the radius of the circle of 95% confidence of the mean pole. K is precision parameter of the paleopole.

fluid temperatures (~100°C; Qian et al. 2011). Furthermore, the porphyritic granite boulder samples show the oxidisation of magnetite to hematite (Fig. 8d). The crystallisation of native Ag and Ag-bearing minerals also likely occurred during this stage in relatively low supergene temperature conditions.

The second mineralisation stage indicates again higher temperatures causing crystallisation of chalcopyrite, pyrrhotite, sphalerite, pyrite, and arsenopyrite (Table 1; Fig. 11). The second stage minerals typically contain galena, native Ag and Ag-bearing minerals as inclusions. Additionally, marcasite inclusions enclosed in second stage pyrite was observed in a granite boulder sample (72_758oku; Fig. 12). Further evidence for the fluid evolution is provided by qualitative analysis of sulfidation stages using reflected microscopy (Fig. 13). Sulfidation state is a function of the temperature and sulphur fugacity (Barton 1970). Variable types of fluid evolution presented in Figure 11 imply that the temperature has changed or the fugacity of sulphur has decreased/increased during the mineralisation process.

5.2. Paleomagnetic evidence for hydrothermal fluid activity

As described above, the Hiekkapohja area shows as a negative total magnetic field anomaly ('aeromagnetic low'), but as a positive Bouguer (gravimetric) anomaly (Fig. 2). The Hiekkapohja granodiorite does not differ in composition or age from the surrounding granodiorites. These features indicate hydrothermal alteration which has reduced the total magnetization (Heilimo & Niemi 2015) and, therefore, the main interest in petrophysical studies was in the magnetic properties of the rocks. Only two of the six paleomagnetic sampling localities provided statistically meaningful remanence directions in the Hiekkapohja region. The obtained directions and paleomagnetic poles calculated from the Soimavuori granite and granitic veins (Soimavuori lithodeme) and Hiekkapohja granodiorite (Muurame lithodeme) correspond to each other within error limits (Table 3). The new poles correspond, within the error limits, to the Svecofennian ca. 1840–1880 Ma paleopoles of Fennoscandia (e.g. Huhma 1981, Elming & Pesonen 2010, Mertanen & Pesonen, 2012, Klein et al. 2016).

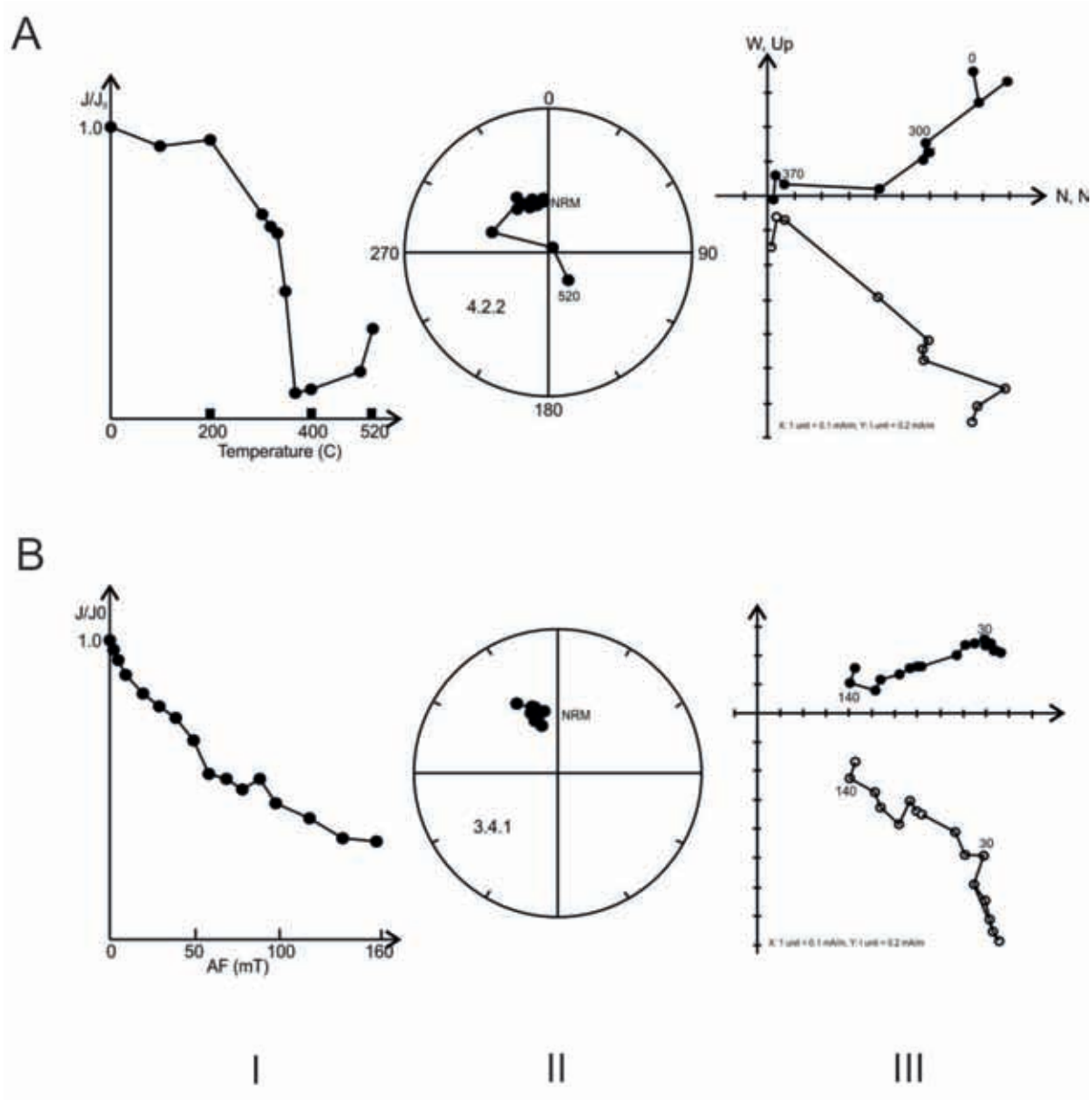

Figure 10 a). Example of thermal demagnetization behavior of sample 4.2.2 from Halsvuori porphyritic granodiorite (Hiekkapohja granodiorite, Muurame lithodeme). Numbers refer to temperatures (°C). b) Example of AF demagnetization behavior of sample 3.4.1 from Soimavuori granite (Soimavuori Lithodeme). Numbers refer to AF fields (mT). (I) intensity decay curve during demagnetization, (II) stereoplot, (III) orthogonal vector plots where open (closed) symbols denote vertical (horizontal) planes.

Both the Soimavuori granite and the Hiekkapohja porphyritic granodiorite are deformed. Thus, the occurrence of a Svecofennian age remanence in them means that the acquisition of remanence must have taken place after the deformation. If blocking of the remanence would have occurred before the deformation, the remanence directions would be scattered. This is the case at the Ankeriasjärvi site (Site 2), outside the aeromagnetic low, where paleomagnetic data from similar deformed

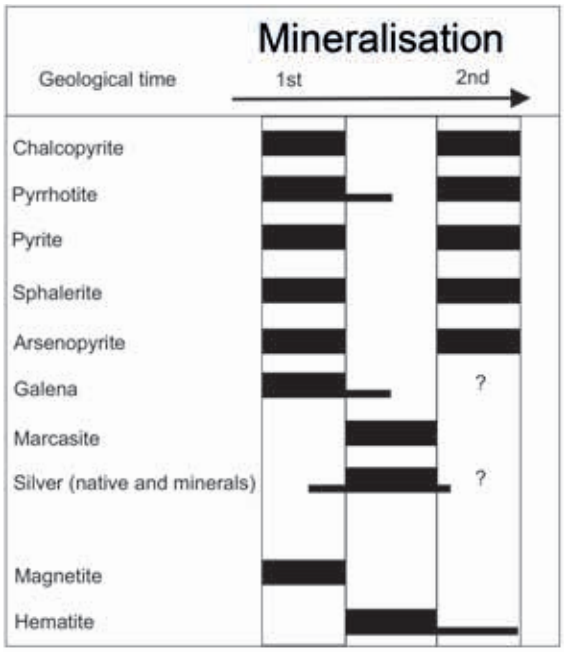

Figure 11. Generalised summary of the major mineral paragenesis in the Hiekkapohja area.

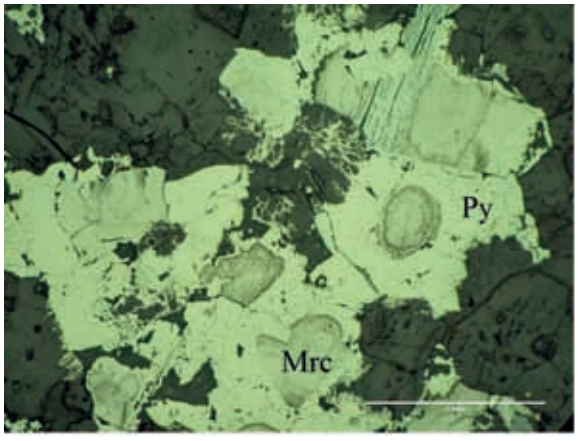

Figure 12. Coarse pyrite (Py) grain surrounding colloform marcasite (Mrc) in granite boulder sample (72_758oku.) Microscope photo with reflective light and parallel nicols.

porphyritic granite are scattered. Post-tectonic resetting of remanence within the aeromagnetic low suggests that the resetting of remanence and the local aeromagnetic anomaly are connected. The age of the Hiekkapohja granodiorite (authors' unpublished age 1882 ± 4 Ma) overlaps with the age of the Soimavuori granite (authors' unpublished age 1879 ± 4 Ma). However, based on the field evidence the age relationship is clear (Fig. 3a).The similarity of the remanence and the petrophysical features suggests that both the Soimavuori and the Hiekkapohja granitoids have experienced equal hydrothermal event(s) that is also evidenced by the dissolution magnetite observed in thin sections from Soimavuori.

5.3 Mineralisation style and history in the Hiekkapohja area

The Hiekkapohja area exhibits several features typical for porphyry-type mineralisations: (1) a circular area containing the mineralised outcrops, (2) bedrock consisting mainly of granitoids, (3) shear systems, that have likely contributed to the multiple mineralisation events and (4) variable enrichment of metals (e.g. Sillitoe 2010). The typical porphyry deposits display zoning of enriched elements from core outwards: Cu-Mo, Pb-Zn, and peripheral Au-As. The Hiekkapohja area shows signs of a similar zoning (Fig. 2). Nonetheless, some of the indications are from boulder samples with uncertain transport distances, which increases uncertainty of the interpretations. Sheared nature of the mineralised locations suggest that the shear systems might have provided pathways for the migrating fluids during the mineralization events.

Modern porphyry systems are typically several cubic kilometers in size, and their alternation patterns, metalliferous elements and alteration types form circular zones or radial dike swarms outwards from the center. The igneous activity typically comprises several generations of intermediate to felsic porphyry intrusions. The younger Soimavuori granite and related dykes in the Hiekkapohja area might represent features favourable for a 'porphyry system' as the source for fluids and heat (Fig. 2). In the Phanerozoic porphyry systems, the progressive thermal decline of the systems has resulted in the characteristic overprinting and partial to total reconstitution of older alteration and mineralisation types by

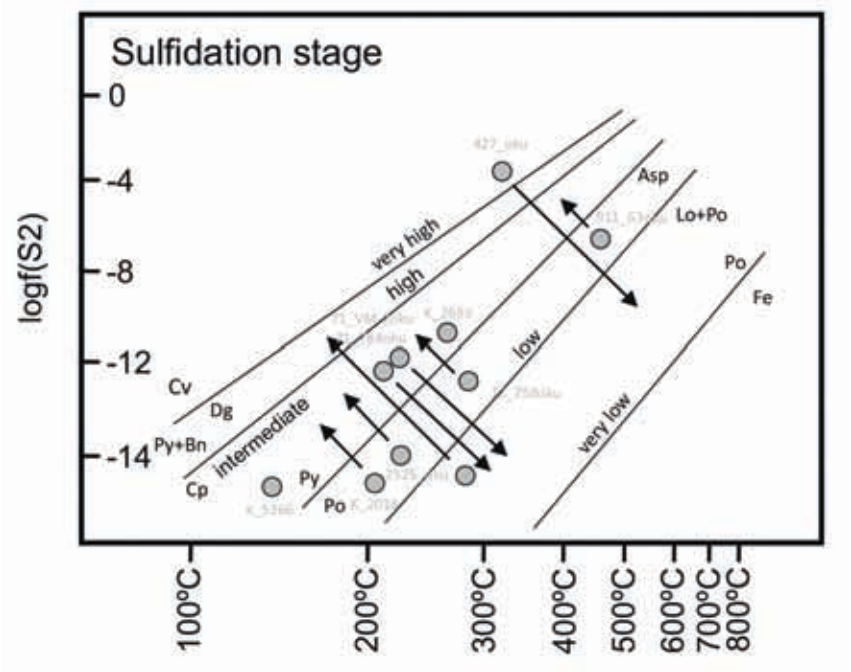

Figure 13. Estimated fluid evolution as sulfidation stages (after Barton 1970) based on qualitative mineralogical observations from the studied samples made using reflected light microscope. The arrows indicate fluid evolution. Abbreviations: Cv – covellite, Dg – digenite, Py – pyrite, Bn – bornite, Cp – chalcopyrite, Po – pyrrhotite, Asp – arsenopyrite, Lo – löllingite, Fe – iron.

younger ones (Sillitoe 2010). The paragenesis of the ore minerals in the Hiekkapohja ore showings is an evidence of a multistage fluid generation in the area (Fig. 11). Also, the sulfidation stages of the mineralised samples indicate a complex evolution for mineralisations (Fig. 13).

The Hiekkapohja granodiorite does not differ in composition or age from the surrounding granodiorites. (i) The first stage mineralisation is likely related to an extensive alteration process as all the known mineralised deposits concentrate within the wide area of altered bedrock. (ii) The low temperature oxidising event possibly created the large circular aeromagnetic low related to alteration of pyrrhotite and magnetite. The resetting of the magnetic remanence within the aeromagnetic low suggests that these two features are connected. We propose that this alteration event, would have also reset the paleomagnetic pole of the Hiekkapohja area to the observed Svecofennian directions. (iii) In the second mineralisation stage hydrothermal fluids caused partial remobilisation of Cu and other base metals and, increased metal concentrations locally. Evidence for the second higher temperature stage are the marcasite and silver inclusions inside the second stage ore minerals (Figs. 8, 11). The regional, 120°–135° trending shear zone is probably clearly younger than the hydrothermal fluids forming the aeromagnetic low (Fig. 2; Mikkola et al. 2016).

If the origin of mineralisations would be related only to fluid flow along shear zones, it would be difficult to explain their the more frequent occurrence (as boulders and outcrops) in the Hiekkapohja area compared to the rest of the 40 000 km^2 belonging to the CFGC. Neither does this theory explain the formation of the circular aeromagnetic low. Furthermore, obscuring of the majority of the paleomagnetic poles suggests a widespread fluid activity occurring (temporally?) close to the peak of granite emplacement.

6. Concluding remarks

1) The small mineralisations in the Hiekkapohja area formed via complex and multiphase hydrothermal alteration. At least two high temperature hydrothermal alteration stages separated by low temperature oxidising stage can be identified.

2) Based on the stable paleomagnetic data from two of the sampling sites, the hydrothermal alteration has taken place after the main deformation of the Hiekkapohja area.
3) The proposed mineralisation and alteration history can be summarised as follows:
   a. Stage 1: a widespread alteration and mineralisation event creating the circular distribution of the mineralisations.
   b. Oxidising stage: relative low temperature stage crystallised native Ag and Ag bearing minerals as well as altered pyrrhotite and chalcopyrite to colloform marcasite as well as magnetite to hematite. Alteration of pyrrhotite and magnetite caused the aeromagnetic low.
   c. Stage 2: high temperature mineralisation enclosed native Ag and Ag bearing minerals as well as the colloform marcasite as inclusions in other ore minerals. The migration of the hydrothermal fluids was controlled by the 120°–135° trending fault zones during this stage.
4) The metalliferous fluid activity stages and overall geological setting in Hiekkapohja resemble those characterising modern porphyry systems.

Supplementary data

Electronic Appendices are available via Bulletin of the Geological Society Finland web page.
Electronic Appendix A: Compiled whole-rock major, trace and precious element data from Hiekkapohja area
Electronic Appendix B: Paleomagnetic methods
Electronic Appendix C: Paleomagnetic site descriptions

Acknowledgements

We would like to thank all those who participated in the field and laboratory work and especially Bo Johanson for the SEM analyses. Kalevi Rasilainen, Edward Lynch, Shenghong Yang and Jarmo Kohonen are thanked for improving the manuscript and Maarit Kalliokoski for polishing the English language. We would also like to acknowledge the late Aimo Hartikainen, who during our prolonged project was the first one to say: ”Hiekkapohja could be a porphyry type system”.

References

Barton, P.B.Jr. 1970. Sulfide Petrology. Mineralogical Society of America Special Paper 3, 187–198.

Boynton, W.V. 1984. Geochemistry of Rare Earth Elements: Meteorite Studies. In: Henderson, P., Ed., Rare Earth Element Geochemistry, Elsevier, New York, 63–114.

Elming, S.-Å. & Pesonen, L.J. 2010. Recent Developments in Paleomagnetism and Geomagnetism. Sixth Nordic Paleomagnetic Workshop, Luleå (Sweden), 15–22 September 2009. EOS, 90 (51) 502.

Fisher, R.A., 1953. Dispersion on a sphere. Proceedings of the Royal Society of London 217, 295–305.

Frost, B.R., Barnes, C.G., Collins, W.J., Arculus, R.J., Ellis, D.J. & Frost, C.D. 2001. A geochemical classification for granitic rocks. Journal of Petrology 42, 2033–2048. https://doi.org/10.1093/petrology/42.11.2033

Halonen, S. 2015. Keski-Suomen granitoidikompleksin malmiviitteet Hiekkapohjan alueella. Master thesis, Oulu mining school, 100 p. (In Finnish, unpublished)

Hangala, S.K. 1982. The plutonic rocks and the associated ore mineralizations at Palokka, Jyväskylä, central Finland. Master's thesis, University of Helsinki, the Department of geology and mineralogy, 58 p. (unpublished)

Heilimo, E. & Niemi, S. 2015 Geokemialliset maaperätutkimukset ja geofysikaaliset maastomittaukset Hiekkapohjan alueella Jyväskylässä ja Laukaassa. Geological Survey of Finland Archive report 74/2015, 13 p. (In Finnish with English abstract)

Heilimo, E. Ahven, M. & Mikkola, P. 2018. Central Finland granitoid complex igneous rocks geochemistry. Geological Survey of Finland, Bulletin 407, 106–129. https://doi.org/10.30440/bt407.6

Huhma, A. 1981. Youngest Precambrian dyke rocks in North Karelia, East Finland. Geological Society of Finland, Bulletin 53, 67–82.

Huhma, H. 1986. Sm–Nd, U–Pb and Pb–Pb isotopic evidence for the origin of the Early Proterozoic Svecokarelian crust

in Finland. Geological Survey of Finland, Bulletin 337, 48 p.

Ikävalko, O. 1981. Malmitutkimukset Jyväskylän alueella kesällä 1981. Geological Survey of Finland, Archive report M19/3212 06/81/1/10, 25 p.

Ikävalko, O. 1983. Tutkimus moreenin maannosprofiilin B-horisontin arseenigeokemian soveltuvuudesta malminetsintämenetelmäksi käytettäessä puolikvantitatiivista (Gutzeitin) analyysimenetelmää Jyväskylän mlk:n Palokan aluella. Geological Survey of Finland, Archive report M16/3212/-83/1/30, 25 p. (In Finnish)

Ikävalko, O. 1984. Jyväskylän mlk:n Sulunperän molybdeeniaiheen tutkimukset vuosina 1982 – 1983. Geological Survey of Finland, Archive report M19/3212/-84/1/10, 21 p. (In Finnish)

Ikävalko, O. 1986a. Jyväskylän mlk:n Riuttamäen ympäristön arseenikiisumineralisaatioiden tutkimuksista 1981–1983. Geological Survey of Finland, Archive report M19/3212 06/-86/2/10. 9 p. (In Finnish)

Ikävalko, O. 1986b. Jyväskylän mlk:n Sulunperän molybdeenitutkimukset, jatkoraportti. Geological Survey of Finland, Archive report M19/3212/-86/3/10, 1 p. (In Finnish)

Kesler, S.E. & Wilkinson, B.H. 2008. Earth's copper resources estimated from tectonic diffusion of porphyry copper deposits. Geology 36, 255–258. https://doi.org/10.1130/G24317A.1

Klein, R., Pesonen, L.J., Mänttäri, I. & Heinonen, J.S. 2016. A late Paleoproterozoic key pole for the Fennoscandian Shield: A paleomagnetic study of the Keuruu diabase dykes, Central Finland. Precambrian Research 286, 379–397. https://doi.org/10.1016/j.precamres.2016.10.013

Laitakari, A.J. 1985. Tutkimukset Jyväskylän mlk:ssa, Korttajärven kylässä, valtausalueella Riuttamäki 1 kaivosrekisteri No 3235/1. Geological Survey of Finland Archive report, M06/3212/-85/1/10. 9 p. (In Finnish)

Lahtinen, R., Korja, A. & Nironen, M. 2005. Palaeoproterozoic tectonic evolution of the Fennoscandian shield. In**:** M. Lehtinen, P. Nurmi, T. Rämö (Eds.), The Precambrian Bedrock of Finland — Key to the Evolution of the Fennoscandian Shield, Elsevier Science B.V pp. 418–532.

Lahtinen, R., Huhma, H., Lahaye, Y., Lode, S., Heinonen, S., Sayab, M. & Whitehouse, M.J. 2016. Paleoproterozoic magmatism across the Archean-Proterozoic boundary in central Fennoscandia: Geochronology, geochemistry and isotopic data (Sm–Nd, Lu–Hf, O). Lithos 262, 507–525. https://10.1016/j.lithos.2016.07.014

Lehtonen, M. & Kortelainen, N. 2010. Virttaankankaan maaperänäytteiden mineralogisia määrityksiä SEM-EDS-laitteistolla. Geological Survey of Finland Archive report M41.2/2010/33, 9 p. (In Finnish)

Mertanen, S. & Pesonen, L. 2012. Paleo-mesoproterozoic assemblages of continents: Paleomagnetic evidence for near equatorial supercontinents. Lecture Notes in Earth Sciences 137, 11–35. https://doi.org/10.1007/978-3-642-25550-2_2

Mikkola, P., Heilimo, E., Aatos, S., Ahven, M., Eskelinen, J., Halonen, S., Hartikainen, A., Kallio, V., Kousa, J., Luukas, J., Makkonen, H., Mönkäre, K., Niemi, S., Nousiainen, M., Romu, I. & Solismaa, S. 2016. Jyväskylän seudun kallioperä. Summary: Bedrock of the Jyväskylä area. Geological Survey of Finland, Report of Investigation 227, 95 p. (In Finnish with English summary)

Mikkola, P., Heilimo, E., Luukas, J., Kousa, J., Aatos, S., Makkonen, H., Niemi, S., Nousiainen, M., Ahven, M., Romu, I. & Hokka, J. 2018. Geological evolution and structure along the southeast border of the Central Finland Granitoid Complex. Geological Survey of Finland, Bulletin 407, 5–27. https://doi.org/10.30440/bt407.1

Nenonen, K. & Huhta, P. 1983. Maaperägeologinen lausunto Jyväskylän mlk:n Sulunperän molybdeenilohkareen kulkeutumisolosuhteista. Geological Survey of Finland, Raporttitiedosto1687, 3 p. (In Finnish)

Nironen, M. 1997. The Svecofennian Orogen: a tectonic model. Precambrian Research 86, 21–44. https://doi.org/10.1016/S0301-9268(97)00039-9

Nironen, M. 2003. Keski-Suomen granitoidikompleksi. Summary: Central Finland Granitoid Complex – Explonation to a map. Geological Survey of Finland, Report of Investigation 157, 45 p.

Nironen, M. (ed.) 2017. Bedrock of Finland at the scale 1:1 000 000 – Major stratigraphic units, metamorphism and tectonic evolution. Geological Survey of Finland, Special Paper 60, 128 p.

Nironen, M., Elliot, B.A. & Rämö, O.T. 2000. 1.88–1.87 Ga post-kinematic intrusions of the Central Finland Granitoid Complex: A shift from C-type to A-type magmatism during lithospheric convergence. Lithos 53, 37–58. https://doi.org/10.1016/S0024-4937(00)00007-4

Nironen, M., Kousa, J., Luukas, J. & Lahtinen, R. 2016. Geological Map of Finland – Bedrock 1:1 000 000. Geological Survey of Finland.

Nurmi, P.A. 1982. Applications of lithogeochemistry in the search for Proterozoic porphyry·type molybdenum, copper and gold deposits, southern Finland. Geological Survey of Finland, Bulletin 329, 40 p.

Peccerillo, A. & Taylor, S.R. 1976. Geochemistry of eocene calc-alkaline volcanic rocks from the Kastamonu area, Northern Turkey. Contributions to Mineralogy and Petrology 58, 63–81.

Qian, G., Xia, F., Brugger, J., Skinner, W.M., Bei, J., Cren, G. & Pring, A. 2011. Replacement of pyrrhotite by pyrite and marcasite under hydrothermal conditions up to 220 degrees C: An experimental study of reaction textures and mechanisms. American Mineralogist 96, 1878–1893. https://doi.org/10.2138/am.2011.3691

Rantala, O. 1982. Raportti kallioperäkartoituksesta Jyväskylän kaupungin Palokankaalla kesällä 1982. Outokumpu Oy Malminetsintä 020/3212 05/OPR/82, 4 p. (In Finnish)

Rasilainen, K., Lahtinen, R. & Bornhorst, T. J. 2007. Rock

Geochemical Database of Finland Manual. Geological Survey of Finland, Report of Investigation 164, 38 p.

Rasilainen, K., Eilu, P., Halkoaho, T., Karvinen, A., Kontinen, A., Kousa, J., Lauri, L., Luukas, J., Niiranen, T., Nikander, J., Sipilä, P., Sorjonen-Ward, P., Tiainen, M., Törmänen, T. & Västi, K. 2014. Quantitative assessment of undiscovered resources in volcanogenic massive sulphide deposits, porphyry copper deposits and Outokumpu-type deposits in Finland. Geological Survey of Finland, Report of Investigation 208, 60 p.

Rämö, O.T., Vaasjoki, M., Mänttäri, I., Elliott, B.A. & Nironen, M. 2001. Petrogenesis of the post-kinematic magmatism of the Central Finland granitoid complex I; radiogenic isotope constraints and implications for crustal evolution. Journal of Petrology 42, 1971–1993. https://doi.org/10.1093/petrology/42.11.1971

Sillitoe, R.H. 2010. Porphyry Copper Systems. Economic Geology 105, 3–41. https://doi.org/10.2113/gsecongeo.105.1.3

Solismaa, S., Niemi, S., Heilimo, E., Nenonen, J. & Kousa, J. 2018. Indications of a Cu-Au mineralisation at Lammuste, central Finland. Geological Survey of Finland, Bulletin 407, 151–167. http://tupa.gtk.fi/julkaisu/liiteaineisto/bt_407_appendix_1.pdf

Tiainen, M., Molnar, F. & Koistinen, E. 2013. The Cu-Mo-Au mineralisation of the Paleoproterozoic Kedonojankulma intrusion, Häme Belt, Southern Finland. 12th Biennial SGA Meeting Uppsala, Sweden, vol. 2, 892–895.

Virtanen, V.J. & Heilimo, E. 2018. Petrogenesis of the geochemically A-type Saarijärvi suite, evidence for bimodal magmatism. Geological Survey of Finland, Bulletin 407, 130–150. https://doi.org/10.30440/bt407.7

Wanhainen, C., Billström, K. & Martinsson, O. 2006. Age, petrology and geochemistry of the porphyritic Aitik intrusion, and its relation to the disseminated Aitik Cu-Au-Ag deposit, northern. GFF 128, 273–286. https://doi.org/10.1080/11035890601284273